

Residual pattern of the hyperintense area on T2-weighted magnetic resonance imaging after initial treatment predicts the pattern and location of recurrence in patients with newly diagnosed glioblastoma

Yoshiteru Shimoda

Tohoku University Graduate School of Medicine

Masayuki Kanamori (✉ mkanamori@med.tohoku.ac.jp)

Tohoku University Graduate School of Medicine

Shota Yamashita

Tohoku University Graduate School of Medicine

Ichiyo Shibahara

Kitasato University Graduate School of Medicine

Rei Umezawa

Tohoku University Graduate School of Medicine

Shunji Mugikura

Tohoku University Graduate School of Medicine

Keiichi Jingu

Tohoku University Graduate School of Medicine

Ryuta Saito

Nagoya University Graduate School of Medicine

Yukihiko Sonoda

Yamagata University Graduate School of Medicine

Toshihiro Kumabe

Kitasato University Graduate School of Medicine

Hidenori Endo

Tohoku University Graduate School of Medicine

Case Report

Keywords: glioblastoma, hyperintense area, T2-weighted magnetic resonance imaging, failure pattern

Posted Date: August 28th, 2023

DOI: <https://doi.org/10.21203/rs.3.rs-3286164/v1>

License:  This work is licensed under a Creative Commons Attribution 4.0 International License.

[Read Full License](#)

Abstract

Purpose: This study aimed to investigate the clinical significance of residual hyperintensity on T2-weighted magnetic resonance imaging in patients with glioblastoma (GB) without enhanced lesions at the end of initial treatment with debulking surgery and concomitant radiotherapy and temozolomide.

Methods: Among 185 GB cases, 80 cases without enhanced lesions at the end of initial treatment and without factors modifying the distribution of residual hyperintense area or pattern of recurrence were included. We retrospectively reviewed the relationship of residual hyperintense area after initial treatment with progression-free survival (PFS), overall survival (OS), and pattern of recurrence.

Results: In these 80 cases, the median PFS and OS were 12.0 and 37.5 months, respectively. At the end of initial treatment, 53 (66.3%) cases had residual hyperintense lesions (T2 residual group, T2R), whereas 27 (33.8%) showed no hyperintensity (T2 vanished group, T2V). Based on univariate and multivariate analyses, the residual hyperintense area after initial treatment was not a prognostic factor for PFS or OS. Distant recurrences occurred more frequently in the T2V group than in the T2R group (47.6% vs. 12.8%). In the T2R group, the recurrence site coincided with the residual hyperintense area in 32 (80.0%) of 40 recurrences.

Conclusion: In GB cases without enhanced lesions at the end of initial treatment, the complete disappearance of the residual hyperintense area after initial treatment does not indicate a favorable outcome. Additionally, distant recurrences should be considered in T2V group and local recurrences should be considered in T2R group.

Introduction

Glioblastoma (GB) is one of the most malignant brain tumors. It is recommended to treat such tumors via maximal safe resection of enhanced lesions on gadolinium-enhanced T1-weighted magnetic resonance (MR) imaging (Gd-T1WI) along with adjuvant temozolomide and radiotherapy [1,2]. However, the associated median survival time is only 14.6 months [3]. A reason for this poor outcome is that tumor cells infiltrate into the surrounding brain beyond the enhanced lesion. As 77.8%–87.5% of cases recur within a 3-cm margin of the resected cavity [4,5], local control is important to improve treatment outcomes.

Total resection of enhanced lesions on Gd-T1WI contributes to local control [6]. To improve local control in GB cases undergoing total resection of enhanced lesions, neurosurgical and radiotherapeutic approaches targeting hyperintense areas surrounding enhanced lesions on T2-weighted MR imaging (T2WI) or fluid-attenuated inversion recovery (FLAIR) imaging have been developed. Previous research has shown the advantage of extensive resection of hyperintense areas surrounding enhanced lesions on FLAIR imaging, i.e., “supratotal resection,” [7-10] as well as additional intensified radiotherapy in hyperintense areas on FLAIR imaging [11,12]. However, due to the eloquence and/or large volume of lesions, these treatments can be difficult to perform [7-9,11,13]. For example, according to a

previous study, resection of 90%–100%, >53.3%, and >20% of hyperintense lesions was only achieved in 6.9%, 24.5%, and 66.2% of cases, respectively [8,9]. In 10% of cases, boosting gamma knife radiosurgery in hyperintense lesions caused treatment-related symptoms and a decline in the performance status [12].

To safely and effectively treat hyperintense lesions on T2WI, it is important to identify the high-risk area for recurrence. Preoperative detection of the high-risk area is the most promising approach because the results can be applied to treatment strategies such as extensive resection or intensive radiotherapy [11]. Recent studies have shown that multiparameter MR imaging as well as ^{11}C methionine and ^{18}F -fluoroethyl-L-tyrosine positron emission tomography can accurately predict the recurrence site with a positive predictive value ranging from 60.0% to 79.0% [11,14-16].

In this study, we clarified the significance of residual hyperintense lesions on T2WI in patients with GB who did not have an enhanced lesion at the end of initial treatment with debulking surgery and concomitant radiotherapy and temozolomide. It is hypothesized that the residual hyperintense area on T2WI, which is independent of the enhanced lesion due to residual and progressive disease at the end of initial treatment, reflects the high-risk area for recurrence in newly diagnosed GB cases. Performing estimation at this time point has three main advantages. First, the vasogenic edema caused by the enhanced lesion due to increased permeability of the vasculature and compression of venous drainage [17,18] could be resolved with debulking surgery, followed by radiotherapy and temozolomide administration. Second, estimation after initial treatment can assess not only the distribution of infiltrating tumor cells but also the infiltrating area that is resistant to radiation and temozolomide [19]. Third, improved brain shift caused by the enhanced lesion allows for validation of the anatomical relationship between hyperintense area and recurrence (Supplementary Fig. 1). Based on this hypothesis, we aimed to assess whether the hyperintense area on T2WI after initial treatment can predict the pattern of recurrence and outcome in patients with GB who did not have enhanced lesions due to residual or progressive enhanced disease.

Methods

This retrospective study was approved by the Institutional Review Board committee of Tohoku University Hospital (2021-1-393), and participants were given the option to opt out of this study.

Patients

In this study, patients with adult supratentorial GB with the wild-type isocitrate dehydrogenase gene were recruited according to the World Health Organization classification of central nervous system tumors, 5th edition [20]. These patients had undergone debulking surgery at our department between January 2008 and December 2019, and the follow-up data until March 2022 were analyzed [4,21]. We reviewed T2WI, T1WI, Gd-T1WI, and diffusion-weighted images obtained before resection, within 72 h after resection, at the end of initial treatment, and at recurrence. Based on Gd-T1WI with regard to the findings of diffusion-

weighted images, we determined the clinical significance of the enhanced lesion to discriminate the residual tumor from the surgical damage, including the influence of carmustine wafers, ischemic complications. The linear, rather than nodular, enhancement around the resection cavity was regarded as a reactive change to carmustine wafer implantation [22]. Only patients who did not have residual or progressive enhanced lesions at the end of initial treatment with concomitant radiotherapy and temozolomide were included to investigate the significance of hyperintense areas on T2WI. The enhancement, which highly indicated pseudoprogression, was also excluded due to the difficulty in discriminating it from true progression and the significant edema caused by this entity [23]. Additionally, we excluded cases that showed factors modifying the distribution of hyperintense area on T2WI as shown in Fig. 1.

Treatment and follow-up

All patients received concomitant radiotherapy (60 Gy) and temozolomide (75 mg/m²/day), followed by adjuvant temozolomide. During this period, the hyperintense area on T2WI was included in the radiation field. From January 2008 to September 2013, radiotherapy consisted of 30 Gy of whole-brain radiotherapy (2.0 Gy/fraction), followed by 30 Gy of extended local accelerated hyperfractionated radiotherapy (1.5 Gy/fraction, twice daily) to the primary site. Patients were treated with 60 Gy of radiation to the local site (2.0 Gy/fraction) after October 2013 [18]. Subsequently, patients were administered adjuvant temozolomide until progression, until 12 months in principle even in the absence of progression, and until a maximum of 24 months in the absence of progression. During and after adjuvant temozolomide administration, patients were followed up via MR imaging every 2 months for 3 years and every 3 months thereafter.

Radiological assessment

Based on T2WI and Gd-T1WI findings after initial treatment with concomitant radiotherapy and temozolomide, the patients were classified into two groups: residual hyperintense area on T2WI (T2R) group (cases with a residual hyperintense area around the resection cavity on T2WI) and vanished hyperintense area on T2WI (T2V) group (cases with no hyperintensity on T2WI). Local recurrence indicates lesions located within a 3-cm margin of the resected cavity [4,5], whereas distant recurrence indicates lesions located >3 cm away from the resected cavity margin or leptomeningeal disease.

In the T2R group, the residual hyperintense area on T2WI at the end of initial treatment was compared with the site of recurrence. Based on the anatomical relationship of the newly developed enhanced lesion with the site of the residual hyperintense area on T2WI, the recurrence patterns were divided into three categories: local recurrence within the residual hyperintense area on T2WI (Fig. 2), local recurrence at sites other than the residual hyperintense area on T2WI (Fig. 3), and distant recurrence (Fig. 4). These data were analyzed by two qualified neurosurgeons (Y. Shimoda and M. K.) who were blinded to the patient's clinical data.

Clinical and radiological data

Patient clinical data, including age, sex, tumor location, recursive partitioning analysis classification for GB [24], maximum tumor diameter, and extent of resection, were retrospectively collected from medical records. The methylation status of the O6-methylguanine–methyltransferase (*MGMT*) gene promoter was assessed as previously described [25-27]. Briefly, DNA was extracted using QIAamp DNA Mini Kit (Qiagen, Valencia, U.S.). After sodium bisulfate modification using Methylamp 96 DNA Modification Kit (EpigenTec, Framingdale, U.S.), DNA was amplified via polymerase chain reaction using primer sequences specific to unmethylated or methylated promoter sequences [26]. DNA fragments were separated on 4% agarose gels and visualized with ethidium bromide.

Statistical analysis

Student's *t*-test was used to compare two groups of parametric data; Wilcoxon rank-sum test was used to compare two groups of nonparametric data; Kruskal–Wallis test was used to compare three groups of nonparametric data; and Fisher's exact test was used to compare proportions. Progression was defined as neurological and radiological deterioration requiring salvage or active treatment termination. Progression-free survival (PFS) was defined as the time from the day of debulking surgery to the day of progression or last follow-up without recurrence, whereas overall survival (OS) was defined as the time between the day of debulking surgery and death or last follow-up. To examine the effect of the residual hyperintense lesion on local control, local PFS rates were also compared. They were calculated using Kaplan–Meier survival curves and compared using log-rank test. For multivariate analysis, the Cox proportional hazard model was used to analyze PFS, local PFS, and OS, thus controlling for age, recursive partitioning analysis classification for GB, extent of resection, carmustine wafer implantation, whole-brain radiotherapy, methylation status of *MGMT* promoter, and residual hyperintense area on T2WI at the end of initial treatment. All statistical analyses were performed using JMP Pro 16.0 (SAS Institute Japan Inc., Tokyo, Japan). A two-tailed *p*-value of <0.05 was considered to indicate statistical significance.

Results

Patient characteristics

Between 2008 and 2019, 185 patients underwent debulking surgery for enhanced lesions at our department, with 69 patients having enhanced lesions due to residual or progressive disease or suspected pseudoprogression at the end of initial treatment. All cases did not receive corticosteroid after initial treatment. After excluding 36 cases, 80 cases were included in this study (Fig. 1). The follow-up period ranged from 8.2 to 84.0 (median, 25.4) months. The median PFS and OS were 12.0 and 37.5 months, respectively. The 5-year PFS and OS rates were 18.2% and 26.2%, respectively. These findings suggest that patients who did not have enhanced lesions at the end of their initial treatment showed a favorable prognosis.

Classification based on T2WI and Gd-T1WI images after initial treatment

The T2V and T2R groups included 27 (33.8%) and 53 (66.3%) cases, respectively. The patient clinical characteristics are summarized in Table 1. The distribution of the methylation status of *MGMT* promoter and tumor location varied between the two groups, without any statistically significant difference. The methylated *MGMT* promoter and parietal lesions were frequently observed in the T2R group (Table 1).

Failure pattern in each group

The failure pattern was investigated in both groups. The clinical background and findings are summarized in Supplemental Table 1. In the T2V group, 21 cases (77.8%) showed recurrence at the end of the follow-up period, with local and distant recurrence (Fig. 4) occurring in 11 (52.3%) and 10 (47.6%) cases, respectively. Among patients with distant recurrence, seven patients showed distant parenchymal recurrence, two had leptomeningeal dissemination, and two had ventricle dissemination. In the T2R group, recurrence occurred in 40 cases (75.5%), with local and distant recurrence occurring in 34 (85.0%) and 6 (15.0%) cases, respectively. Among patients with distant recurrence, five patients had distant parenchymal recurrence and one had ventricle dissemination. Local recurrence occurred more frequently in the T2R group than in the T2V group ($p = 0.012$). The anatomical relationship of the residual hyperintense lesion on T2WI with the recurrence site was investigated. Of the 34 local recurrence cases in the T2R group, 32 (94.1%) cases showed recurrence in the region corresponding to the residual hyperintense area on T2WI (Figs. 2 and 3). All recurrences from the hyperintense area were detected within a 3-cm margin of the resected cavity. These findings suggest that the residual hyperintense area on T2WI at the end of initial treatment can predict the pattern and site of recurrence.

Prognostic significance of T2WI findings after initial treatment

To determine the impact of the residual hyperintense area on T2WI images on progression and survival, the PFS, local PFS, and OS were compared between the two groups. The median PFS, local PFS, and OS were 12.6, 13.3, and 37.7 months in the T2R group and 10.0, 16.0, and 28.4 months in the T2V group, respectively, with no statistically significant differences between the two groups ($p = 0.93, 0.44, \text{ and } 0.21$, respectively; Supplementary Fig. 2). As the background, including the methylation status of *MGMT* promoter, differed between the two groups (Table 1), a multivariate analysis using the Cox proportional hazard model was performed. The residual hyperintense area on T2WI was not a prognostic factor for PFS, local PFS, or OS (Supplemental Table 2), suggesting that the residual hyperintense area on T2WI after initial treatment does not indicate poor outcomes.

Discussion

This study evaluated the significance of the residual hyperintense area on T2WI without enhanced lesions at the end of initial treatment with concomitant radiotherapy and temozolomide. When the hyperintense area was present on T2WI, 80.0% of recurrences occurred within the hyperintense lesion. However, when the hyperintense area on T2WI vanished, distant recurrence was frequently observed. The finding of hyperintense lesions on T2WI at the end of initial treatment provides a simple method for predicting the pattern and location of recurrence associated with a high risk. Despite

differences in study design and intervention at the high-risk site, the accuracy of predicting recurrence site in this study was superior to that of ^{11}C -methionine and ^{18}F -fluoroethyl-L-tyrosine positron emission tomography before radiotherapy; preoperative apparent diffusion coefficient map; and preoperative machine learning of T2WI, enhanced T1WI, and apparent diffusion coefficient maps [11,14-16,28].

The distribution of the hyperintense area on T2WI may be modified by the anatomical characteristics of the tumor location; GB nature, including sensitivity to radiation and temozolomide; and initial treatment. In this study, the tumor location and methylation status of *MGMT* promoter differed between the two groups. The hyperintense area did not disappear in 93.3% of parietal lobe lesions. Several recent studies have reported the relationship between tumor location and biological characteristics of GB. In GB cases developing enhanced lesions within 6 months after treatment, true progression often occurred in cases of parietal lobe lesions, whereas pseudoprogression frequently occurred in cases of other lesion locations [29]. These findings could aid in predicting the subsequent clinical course during the early phase of treatment. Further, *MGMT* promoter methylation was observed at a high rate in the T2R group. As *MGMT* methylation was a predictive factor for sensitivity to TMZ, a high proportion of cases with *MGMT* promoter methylation in the T2R group may be a contradictory finding. However, the methylation status of the residual lesion on T2WI was not assessed in this study. Wegner *et al.* collected multiple samples of GB and analyzed the methylation status of *MGMT* promoter. In that study, two of the four cases with *MGMT* promoter methylation also had a lesion with an unmethylated gene promoter within the same tumor [30]. Therefore, the residual hyperintense area may reflect residual lesions after initial treatment due to methylation heterogeneity. The therapeutic factors modifying the hyperintense area include surgical procedures, carmustine wafer implantation, and radiotherapy. Among them, the effect of carmustine wafers should be considered while interpreting the results [31]. According to previous studies, perifocal edema occurred in 12.5%–25% of cases with malignant glioma [32,33], and its volume increased at 1–4 weeks after implantation and decreased at 5–8 weeks to the same level as observed in cases without carmustine wafers [32]. As the timing of evaluation in this study was delayed (approximately 2 months after implantation), the effect of carmustine wafers on the distribution of hyperintense areas may be modest.

Similar to our study, Grossmann *et al.* focused on the residual hyperintense area on FLAIR imaging 3 months after resection and investigated the relationship between the volume of the residual hyperintense area and treatment outcome [19]. Their study differs from the current study in that it included cases with enhanced lesions that appeared 3 months after resection. They revealed that the residual volume of the hyperintense area on FLAIR imaging 3 months after surgery, but not before or immediately after surgery, correlated with prognosis. Their findings were valuable in determining the prognostic significance of the hyperintense lesion 3 months after resection. However, as their study included cases with enhanced lesions due to residual or progressive disease, the obtained prognostic significance may be overestimated. To assess this significance without the influence of enhanced lesions, cases with such enhanced lesions at the end of initial treatment were excluded in the present

study. Consequently, based on univariate or multivariate analysis, the residual hyperintense area at the end of initial treatment did not indicate a worse PFS or OS rate.

The T2R and T2V groups showed the same recurrence time, but the recurrence patterns were significantly different, possibly due to different recurrence mechanisms. In the T2R group, residual hyperintense lesions represent areas of dense tumor cells that are resistant to initial therapy, based on methylation heterogeneity [30]. In contrast, tumors in the T2V group contain sparse but extensive infiltrative cells around the enhanced lesion that are not detectable on T2WI [34], and recurrence develops from infiltrative cells outside the radiation field.

This study has certain limitations. First, the number of cases with distant recurrence was limited. Therefore, we could not identify patient clinical characteristics to predict distant recurrence. These predictors are important to develop personalized strategies to prevent distant recurrence, which leads to poor outcomes [35]. Second, compared with voxel-based quantitative analyses, rigorous estimation was not achieved via qualitative analysis in this study [14,15]. Instead, the timing of initial treatment completion minimized the anatomical displacement (Supplementary Fig. 1), allowing us to elucidate the anatomical relationship between residual hyperintense sites and recurrence.

Based on these findings, second-look surgery, salvage radiotherapy in the residual hyperintense area, or local convection-enhanced delivery of chemotherapeutic agents [36] may improve the local control of GB in the T2R group with minimal complications. Additionally, novel treatments that focus on preventing distant recurrence rather than local control can improve outcomes in the T2V group. Accordingly, multicenter, prospective studies can reveal definitive and clinical significance of residual hyperintense area on T2WI after treatment as well as provide useful information for developing salvage treatment after initial treatment with radiotherapy and temozolomide for GB.

Conclusions

In this study, 66.3% of cases had a residual hyperintense area on T2WI despite the absence of enhanced lesions due to residual or progressive disease at the end of initial treatment with radiotherapy and temozolomide. This finding did not indicate a poor prognosis. In 80.0% of cases with residual hyperintense areas on T2WI, recurrence occurred within the hyperintense lesion. Distant recurrence occurred more frequently in the T2V group. The finding of T2WI at the end of initial treatment was useful in predicting the pattern and site of recurrence.

Declarations

Funding: None

Competing interests: There are no financial or nonfinancial interests that are directly or indirectly related to the work submitted for publication.

Author contributions:

Conceptualization: Y.Shimoda, MK

Data curation: SY, IS, RU, SM, RS, Y.Sonoda, TK

Analysis of data: Y.Shimoda, MK

Interpretation of data: Y.Shimoda, MK, IS, RU, SM, KJ, RS, Y.Sonoda, TK, HE

Statistical analysis: Y.Shimoda, MK

Writing of the manuscript: Y.Shimoda, MK

Review and discussion of the manuscript: All the authors.

Data availability: NA

Ethics approval: This retrospective study was approved by the Institutional Review Board committee of Tohoku University Hospital (2021-1-393).

Consent to participate and to publish: NA (Participants were given the option to opt out of this study.)

References

1. Sanai N, Polley MY, McDermott MW, Parsa AT, Berger MS (2011) An extent of resection threshold for newly diagnosed glioblastomas. *J Neurosurg* 115:3-8. <https://doi.org/10.3171/2011.2.jns10998>
2. Marko NF, Weil RJ, Schroeder JL, Lang FF, Suki D, Sawaya RE (2014) Extent of resection of glioblastoma revisited: personalized survival modeling facilitates more accurate survival prediction and supports a maximum-safe-resection approach to surgery. *J Clin Oncol* 32:774-782. <https://doi.org/10.1200/JCO.2013.51.8886>
3. Stupp R, Mason WP, van den Bent MJ et al (2005) Radiotherapy plus concomitant and adjuvant temozolomide for glioblastoma. *N Engl J Med* 352:987–996.
4. Shibahara I, Sonoda Y, Saito R, Kanamori M, Yamashita Y, Kumabe T, Watanabe M, Suzuki H, Watanabe T, Ishioka C, Tominaga T (2013) The expression status of CD133 is associated with the pattern and timing of primary glioblastoma recurrence. *Neuro Oncol* 15:1151-1159. <https://doi.org/10.1093/neuonc/not066>
5. Chamberlain MC (2011) Radiographic patterns of relapse in glioblastoma. *J Neurooncol* 101:319-323. <https://doi.org/10.1007/s11060-010-0251-4>
6. Murakami R, Hirai T, Nakamura H, Furusawa M, Nakaguchi Y, Uetani H, Kitajima M, Yamashita Y (2012) Recurrence patterns of glioblastoma treated with postoperative radiation therapy: relationship between extent of resection and progression-free interval. *Jpn J Radiol* 30:193-197. <https://doi.org/10.1007/s11604-011-0031-x>

7. Molinaro AM, Hervey-Jumper S, Morshed RA et al (2020) Association of maximal extent of resection of contrast-enhanced and non-contrast-enhanced tumor with survival within molecular subgroups of patients with newly diagnosed glioblastoma. *JAMA Oncol* 6:495-503
8. Li YM, Suki D, Hess K, Sawaya R (2016) The influence of maximum safe resection of glioblastoma on survival in 1229 patients: can we do better than gross-total resection? *J Neurosurg* 124:977-988. <https://doi.org/10.3171/2015.5.JNS142087>
9. Vivas-Buitrago T, Domingo RA, Tripathi S, De Biase G, Brown D, Akinduro OO, Ramos-Fresnedo A, Sabsevitz DS, Bendok BR, Sherman W, Parney IF, Jentoft ME, Middlebrooks EH, Meyer FB, Chaichana KL, Quinones-Hinojosa A (2022) Influence of supramarginal resection on survival outcomes after gross-total resection of IDH-wild-type glioblastoma. *J Neurosurg* 136:1-8. <https://doi.org/10.3171/2020.10.JNS203366>
10. Wach J, Vychopen M, Kühnapfel A, Seidel C, Güresir E (2023) A systematic review and meta-analysis of supramarginal resection versus gross total resection in glioblastoma: can we enhance progression-free survival time and preserve postoperative safety? *Cancers (Basel)* 15. <https://doi.org/10.3390/cancers15061772>
11. Seidlitz A, Beuthien-Baumann B, Löck S, Jentsch C, Platzek I, Zöphel K, Linge A, Kotzerke J, Petr J, van den Hoff J, Steinbach J, Krex D, Schmitz-Schackert G, Falk M, Baumann M, Krause M (2021) Final results of the prospective biomarker trial PETra: [11C]-MET-accumulation in postoperative PET/MRI predicts outcome after radiochemotherapy in glioblastoma. *Clin Cancer Res* 27:1351-1360. <https://doi.org/10.1158/1078-0432.CCR-20-1775>
12. Duma CM, Kim BS, Chen PV et al (2016) Upfront boost gamma Knife “leading-edge” radiosurgery to FLAIR MRI-defined tumor migration pathways in 174 patients with glioblastoma multiforme: a 15-year assessment of a novel therapy. *J Neurosurg* 125:40-49
13. Kumar N, Kumar R, Sharma SC, Mukherjee A, Khandelwal N, Tripathi M, Miriyala R, Oinam AS, Madan R, Yadav BS, Khosla D, Kapoor R (2020) Impact of volume of irradiation on survival and quality of life in glioblastoma: a prospective, phase 2, randomized comparison of RTOG and MDACC protocols. *Neurooncol Pract* 7:86-93. <https://doi.org/10.1093/nop/npz024>
14. Dasgupta A, Geraghty B, Maralani PJ, Malik N, Sandhu M, Detsky J, Tseng CL, Soliman H, Myrehaug S, Husain Z, Perry J, Lau A, Sahgal A, Czarnota GJ (2021) Quantitative mapping of individual voxels in the peritumoral region of IDH-wildtype glioblastoma to distinguish between tumor infiltration and edema. *J Neurooncol* 153:251-261. <https://doi.org/10.1007/s11060-021-03762-2>
15. Tien RD, Felsberg GJ, Friedman H, Brown M, MacFall J (1994) MR imaging of high-grade cerebral gliomas: value of diffusion-weighted echoplanar pulse sequences. *AJR Am J Roentgenol* 162:671-677. <https://doi.org/10.2214/ajr.162.3.8109520>
16. Buchmann N, Gempt J, Ryang YM, Pyka T, Kirschke JS, Meyer B, Ringel F (2019) Can early postoperative O-(2-18Ffluoroethyl)-l-tyrosine positron emission tomography after resection of glioblastoma predict the location of later tumor recurrence? *World Neurosurg* 121:e467-e474. <https://doi.org/10.1016/j.wneu.2018.09.139>

17. Pietsch T, Valter MM, Wolf HK, von Deimling A, Huang HJ, Cavenee WK, Wiestler OD (1997) Expression and distribution of vascular endothelial growth factor protein in human brain tumors. *Acta Neuropathol* 93:109-117. <https://doi.org/10.1007/s004010050591>
18. Strugar J, Rothbart D, Harrington W, Criscuolo GR (1994) Vascular permeability factor in brain metastases: correlation with vasogenic brain edema and tumor angiogenesis. *J Neurosurg* 81:560-566. <https://doi.org/10.3171/jns.1994.81.4.0560>
19. Grossman R, Shimony N, Shir D, Gonen T, Sitt R, Kimchi TJ, Harosh CB, Ram Z (2017) Dynamics of FLAIR volume changes in glioblastoma and prediction of survival. *Ann Surg Oncol* 24:794-800. <https://doi.org/10.1245/s10434-016-5635-z>
20. Louis DN, Ohgaki H, Wiestler OD, Cavenee WK, Ellison DW, Figarella-Branger D, Reifenberger G, von Deimling A (2016) WHO classification and grading of tumours of the central nervous system. IARC Press, International Agency for Research on Cancer, Lyon
21. Kumabe T, Saito R, Kanamori M, Chonan M, Mano Y, Shibahara I, Kawaguchi T, Kato H, Yamashita Y, Sonoda Y, Kawagishi J, Jokura H, Watanabe M, Katakura R, Kayama T, Tominaga T (2013) Treatment results of glioblastoma during the last 30 years in a single institute. *Neurol Med Chir (Tokyo)* 53:786-796. <https://doi.org/10.2176/nmc.0a2013-0212>
22. Giese A, Kucinski T, Knopp U, Goldbrunner R, Hamel W, Mehdorn HM, Tonn JC, Hilt D, Westphal M (2004) Pattern of recurrence following local chemotherapy with biodegradable carmustine (BCNU) implants in patients with glioblastoma. *J Neurooncol* 66:351-360. <https://doi.org/10.1023/b:neon.0000014539.90077.db>
23. Young JS, Al-Adli N, Scotford K, Cha S, Berger MS (2023) Pseudoprogression versus true progression in glioblastoma: what neurosurgeons need to know. *J Neurosurg*:1-12. <https://doi.org/10.3171/2022.12.JNS222173>
24. Li J, Wang M, Won M, Shaw EG, Coughlin C, Curran WJ, Mehta MP (2011) Validation and simplification of the Radiation Therapy Oncology Group recursive partitioning analysis classification for glioblastoma. *Int J Radiat Oncol Biol Phys* 81:623-630. <https://doi.org/10.1016/j.ijrobp.2010.06.012>
25. Hegi ME, Diserens AC, Gorlia T, Hamou MF, de Tribolet N, Weller M, Kros JM, Hainfellner JA, Mason W, Mariani L, Bromberg JE, Hau P, Mirimanoff RO, Cairncross JG, Janzer RC, Stupp R (2005) MGMT gene silencing and benefit from temozolomide in glioblastoma. *N Engl J Med* 352:997-1003. <https://doi.org/10.1056/NEJMoa043331>
26. Sonoda Y, Kumabe T, Watanabe M, Nakazato Y, Inoue T, Kanamori M, Tominaga T (2009) Long-term survivors of glioblastoma: clinical features and molecular analysis. *Acta Neurochir (Wien)* 151:1349-1358. <https://doi.org/10.1007/s00701-009-0387-1>
27. Sonoda Y, Yokosawa M, Saito R, Kanamori M, Yamashita Y, Kumabe T, Watanabe M, Tominaga T (2010) O(6)-Methylguanine DNA methyltransferase determined by promoter hypermethylation and immunohistochemical expression is correlated with progression-free survival in patients with glioblastoma. *Int J Clin Oncol* 15:352-358. <https://doi.org/10.1007/s10147-010-0065-6>

28. Matsuda K, Kokubo Y, Kanemura Y, Kanoto M, Sonoda Y (2022) Preoperative apparent diffusion coefficient of peritumoral lesion associate with recurrence in patients with glioblastoma. *Neurol Med Chir (Tokyo)* 62:28-34. <https://doi.org/10.2176/nmc.oa.2021-0182>
29. Ismail M, Hill V, Statsevych V, Mason E, Correa R, Prasanna P, Singh G, Bera K, Thawani R, Ahluwalia M, Madabhushi A, Tiwari P (2020) Can tumor location on pre-treatment MRI predict likelihood of pseudo-progression vs. tumor recurrence in glioblastoma?-A feasibility study. *Front Comput Neurosci* 14:563439. <https://doi.org/10.3389/fncom.2020.563439>
30. Wenger A, Ferreyra Vega S, Kling T, Bontell TO, Jakola AS, Carén H (2019) Intratumor DNA methylation heterogeneity in glioblastoma: implications for DNA methylation-based classification. *Neuro Oncol* 21:616-627. <https://doi.org/10.1093/neuonc/noz011>
31. Shibahara I, Miyasaka K, Sekiguchi A, Ishiyama H, Inukai M, Yasui Y, Watanabe T, Sato S, Hide T, Kumabe T (2021) Long-term follow-up after BCNU wafer implantation in patients with newly diagnosed glioblastoma. *J Clin Neurosci* 86:202-210. <https://doi.org/10.1016/j.jocn.2021.01.037>
32. Hasegawa Y, Iuchi T, Sakaida T, Yokoi S, Kawasaki K (2016) The influence of carmustine wafer implantation on tumor bed cysts and peritumoral brain edema. *J Clin Neurosci* 31:67-71. <https://doi.org/10.1016/j.jocn.2015.12.033>
33. Aoki T, Nishikawa R, Sugiyama K et al (2014) A multicenter phase I/II study of the BCNU implant (Gliadel®) Wafer) for Japanese patients with malignant gliomas. *Neurol Med Chir (Tokyo)* 54:290-301
34. Matsuo M, Miwa K, Tanaka O, Shinoda J, Nishibori H, Tsuge Y, Yano H, Iwama T, Hayashi S, Hoshi H, Yamada J, Kanematsu M, Aoyama H (2012) Impact of [11C]methionine positron emission tomography for target definition of glioblastoma multiforme in radiation therapy planning. *Int J Radiat Oncol Biol Phys* 82:83-89. <https://doi.org/10.1016/j.ijrobp.2010.09.020>
35. Konishi Y, Muragaki Y, Iseki H, Mitsunashi N, Okada Y (2012) Patterns of intracranial glioblastoma recurrence after aggressive surgical resection and adjuvant management: retrospective analysis of 43 cases. *Neurol Med Chir (Tokyo)* 52:577-586. <https://doi.org/10.2176/nmc.52.577>
36. Saito R, Kanamori M, Sonoda Y, Yamashita Y, Nagamatsu K, Murata T, Mugikura S, Kumabe T, Wembacher-Schröder E, Thomson R, Tominaga T (2020) Phase I trial of convection-enhanced delivery of nimustine hydrochloride (ACNU) for brainstem recurrent glioma. *Neurooncol Adv* 2:vdaa033. <https://doi.org/10.1093/oaajnl/vdaa033>

Table

Table 1. Clinical characteristics of 80 cases with no enhanced areas at the end of the initial treatment with radiation and temozolomide

		Total	T2V group (<i>n</i> = 27)	T2R group (<i>n</i> = 53)	<i>P</i> - value
Number of cases (%)		80	27 (33.8)	53 (66.2)	
Age at the initial treatment (years)	Mean (SD)	60.2 (13.1)	57.4 (15.6)	61.6 (11.4)	0.18 ^a
Sex (<i>n</i> , %)	Male	46 (57.5)	19 (70.4)	27 (50.9)	0.15 ^b
	Female	34 (42.5)	8 (29.6)	26 (49.1)	
Lesion at the left hemisphere (<i>n</i> , %)	Left	44 (55.0)	14 (51.9)	30 (56.6)	0.80 ^b
	Right	36 (45.0)	13 (48.2)	23 (43.4)	
RPA classification (<i>n</i> , %)	III	9 (11.3)	5 (18.5)	4 (7.8)	0.32 ^b
	IV	26 (32.5)	9 (33.3)	17 (32.1)	
	V	45 (56.3)	13 (48.2)	32 (60.4)	
Extent of resection	GTR	63 (78.8)	20 (74.1)	43 (81.1)	0.47 ^b
	Non-GTR	17 (21.2)	7 (25.9)	10 (18.9)	
Implantation of carmustine wafers	Yes	27 (33.7)	7 (25.9)	20 (37.7)	0.33 ^b
	No	53 (66.3)	20 (74.1)	33 (62.3)	
Methylation status of the <i>MGMT</i> gene promoter (<i>n</i> , %)*	Methylated	43 (55.8)	10 (37.5)	33 (63.5)	0.087 ^b
	Unmethylated	34 (44.2)	15 (62.5)	19(36.5)	
Tumor maximal diameter (mm)	mean (SD)	47.4 (15.8)	48.9 (17.5)	46.7 (15.1)	0.56 ^c
Tumor location (<i>n</i> , %)	Frontal	23	8 (30)	15	0.085 ^b

		(28.8)		(28.3)
	Temporal	35 (43.8)	15 (55.6)	20 (37.7)
	Parietal	15 (18.8)	1 (3.7)	14 (26.4)
	Occipital	3 (3.8)	1 (3.7)	2 (3.8)
	Others	4 (5.0)	2 (7.4)	2 (3.8)

Abbreviations: RPA, recursive partitioning analysis; *MGMT*, O6-methylguanine-methyltransferase; SD, standard deviation; GTR, gross total resection of the enhanced lesion; T2V and T2R, vanished and residual hyperintense areas on T2-weighted magnetic resonance imaging at the completion of initial treatment with radiation and temozolomide, respectively; a, Student's *t*-test; b, Fisher's exact test; c, Wilcoxon rank-sum test; *, data for *MGMT* methylation status were missing in three cases.

Figures

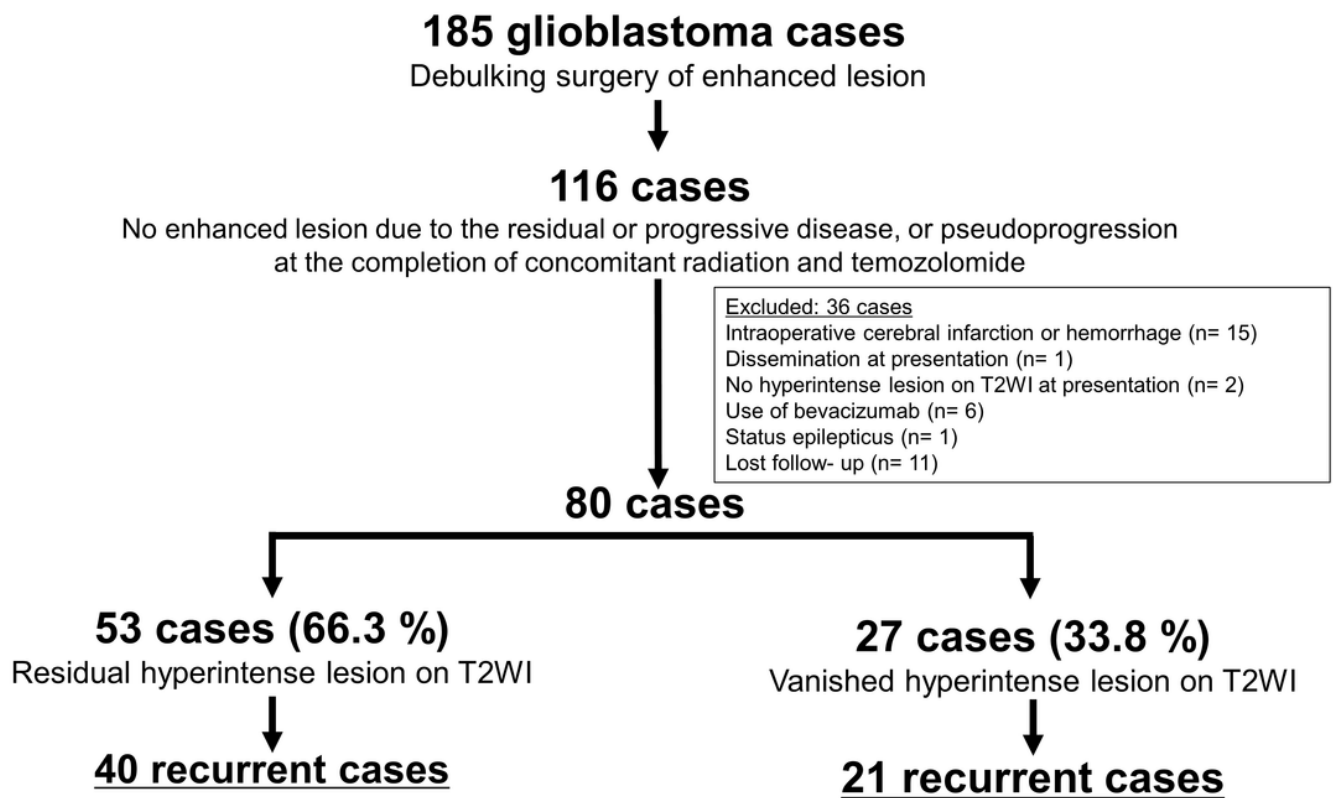


Figure 1

Patient selection criteria for this study

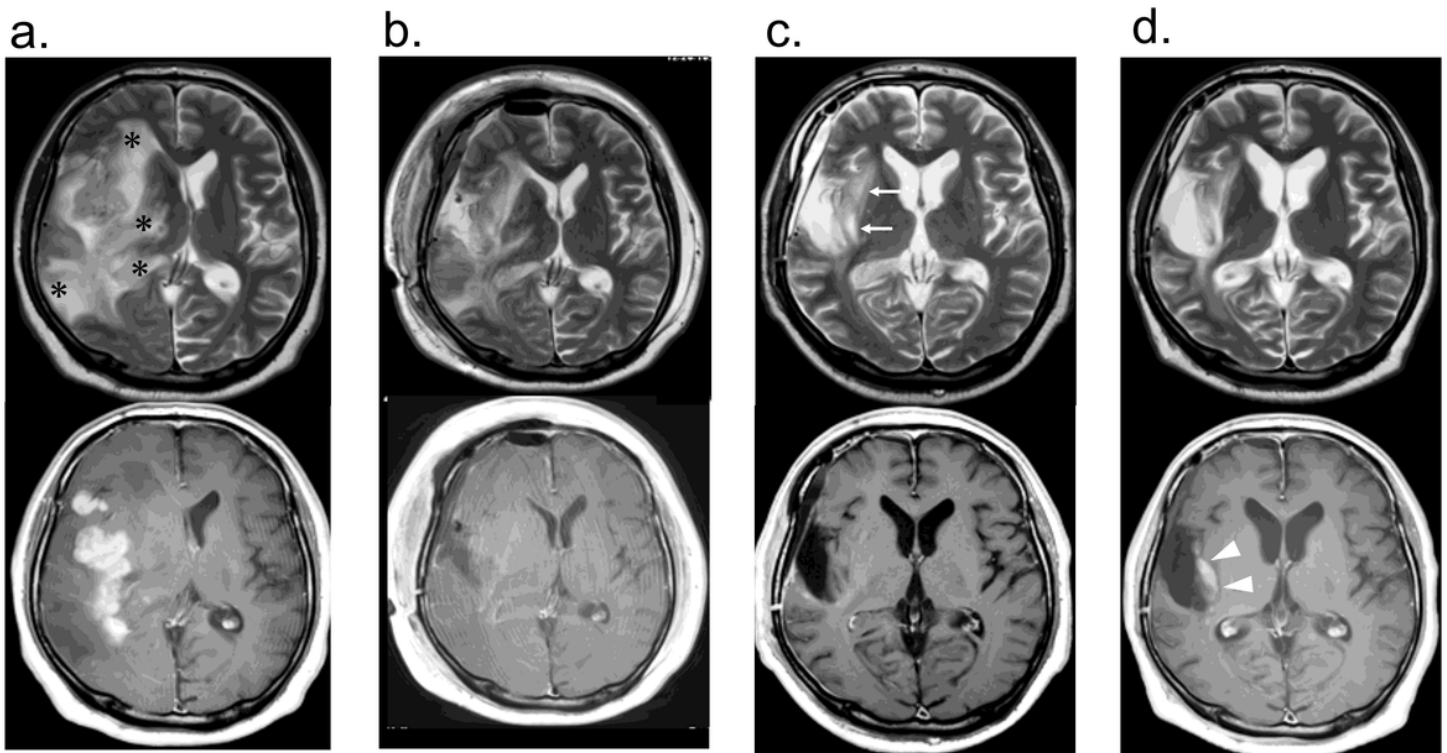


Figure 2

A representative case of local recurrence occurred within the residual hyperintense area on T2-weighted magnetic resonance imaging (T2WI) after initial treatment with radiotherapy and temozolomide

A 60-year-old man was diagnosed with right temporal glioblastoma. T2WI (upper panels) and gadolinium-enhanced T1WI (Gd-T1WI; lower panels) are shown before (a) and immediately after total resection of the enhanced lesion (b), completion of initial treatment (c), and recurrence 5 months after tumor resection (d). Asterisks in A indicate the hyperintense area that diminished after initial treatment with radiotherapy and temozolomide. The arrows in (c) and arrowheads in (d) represent the residual hyperintense area on T2WI after initial treatment and newly developed enhanced area at recurrence, respectively.

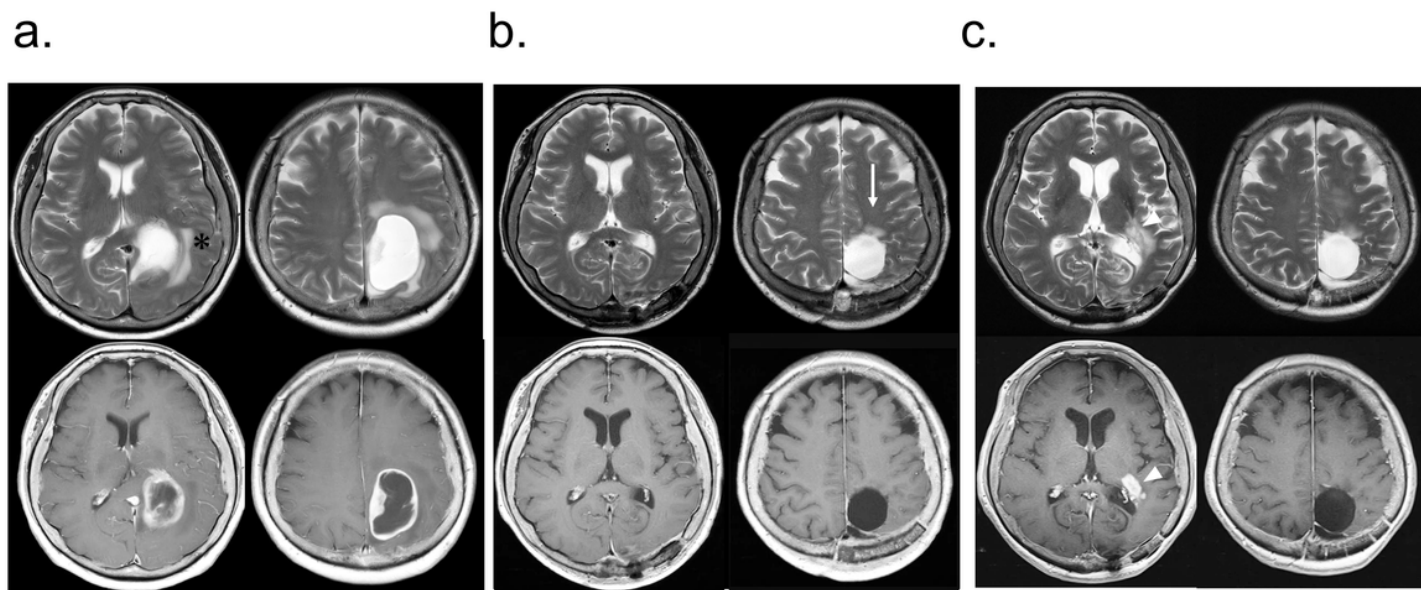


Figure 3

A representative case of local recurrence in a region other than the residual hyperintense area on T2-weighted magnetic resonance imaging (T2WI) after initial treatment

A 62-year-old woman was diagnosed with left parietal glioblastoma. T2WI (upper panels) and gadolinium-enhanced T1WI (Gd-T1WI; lower panels) are shown before surgery (a), after completion of initial treatment (b), and recurrence at 26 months after tumor resection (c). The arrows in (b) and arrowheads in (c) represent the residual hyperintense area on T2WI after initial treatment and newly developed enhanced area at recurrence, respectively. The anatomical location of the residual hyperintense area at the end of initial treatment and recurrence was inconsistent.

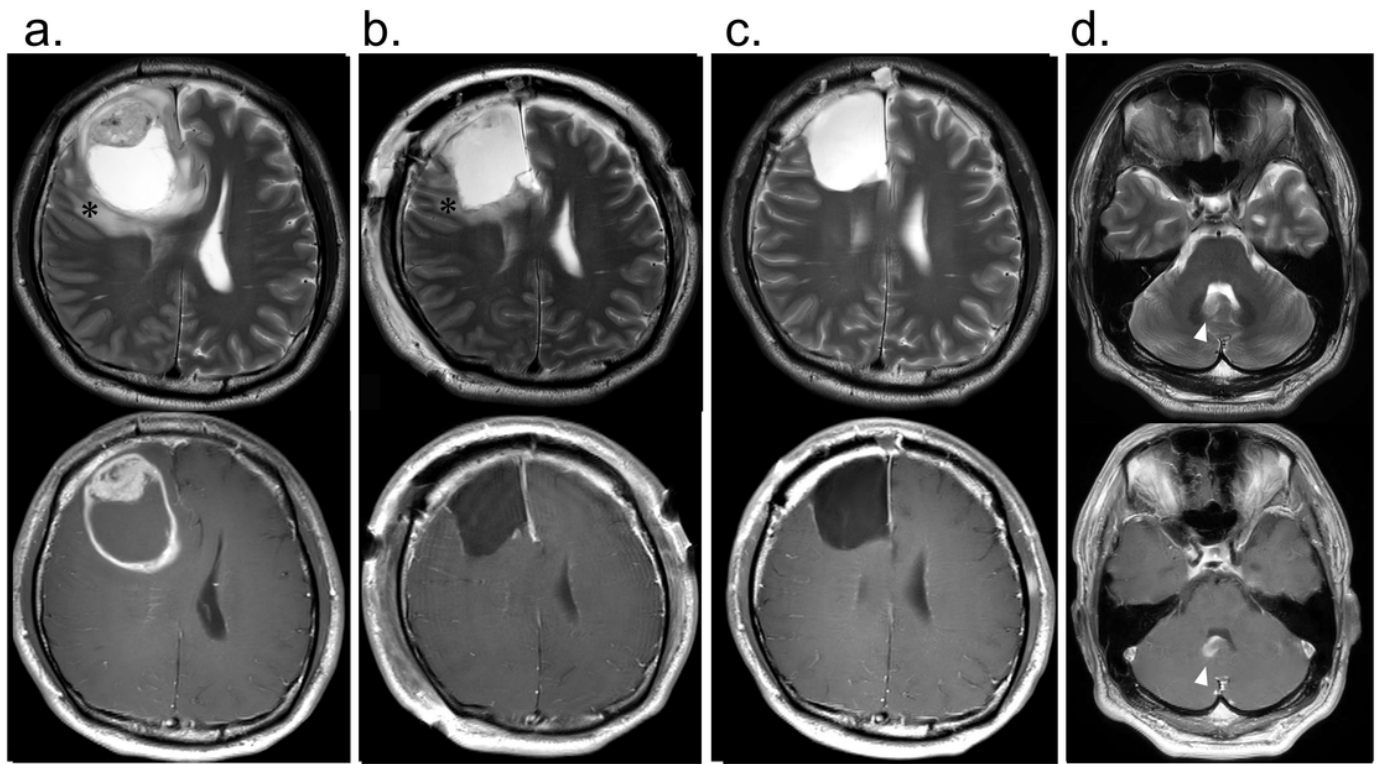


Figure 4

A representative case with a hyperintense area on T2WI that completely vanished after initial treatment with radiotherapy and temozolomide, followed by the development of distant recurrence

A 37-year-old man was diagnosed with left temporal glioblastoma. T2WI (upper panels) and gadolinium-enhanced T1WI (Gd-T1WI; lower panels) are shown before (a) and immediately after total resection of the enhanced lesion (b), completion of initial treatment with radiotherapy and temozolomide (c), and recurrence 5 months after tumor resection (d). The hyperintense area on T2WI completely vanished (asterisks in a and b), and a distant recurrence developed at the cerebellum (arrowheads).

Supplementary Files

This is a list of supplementary files associated with this preprint. Click to download.

- [ShimodaetalSupplementalfile.docx](#)
- [Shimodaetal.SuopplementalTables.docx](#)